EPJ manuscript No.
(will be inserted by the editor)

Photo-elastic properties of the wing imaginal disc of Drosophila

T. Schluck[1] and C. M. Aegerter[1],[2]

[1] Physics Institute, University of Zurich, Winterthurerstr. 190, 8057 Zurich, Switzerland
[2] Fachbereich Physik, Universität Konstanz, Universitätsstrasse 10, 78457 Konstanz, Germany

Received: March 16, 2010/ Revised version: date

Abstract In the study of developmental biology, the physical properties and constraints of the developing tissues are of great importance. In spite of this, not much is known about the elastic properties of biologically relevant tissues that are studied in biology labs. Here, we characterize properties of the wing imaginal disc of Drosophila, which is a precursor organ intensely studied in the framework of growth control and cell polarity. In order to determine the possibility of measuring mechanical stresses inside the tissue during development, we quantify the photo-elastic properties of the tissue by direct mechanical manipulation. We obtain a photo-elastic constant of $2\times10^{-10}\mathrm{Pa}^{-1}$.

PACS. 78.20.Fm Birefringence – 87.85.J- Biomaterials – 87.19.lx Development and growth – 87.80.Fe Micromanipulation of biological structures

1 Introduction

Since the time of D'Arcy Wentworth Thompson, the physical constraints on a developing organism have been taken to strongly influence the growth and shape of the final organism (1). Recently, many specific instances have been found, where mechanical effects influence cell differentiation and growth control in developmental biology (2). This ranges from the formation of shoots in plant growth (3), to the network formation of tubes in the tracheal system of Drosophila (4), to bone calcification (5) or the cell specification in the formation of joints (6). While there is a host of information on genetic influences in all of these systems, the corresponding mechanical properties are not well characterized and only in very few cases have they been determined experimentally (7; 8; 9). In addition, during the development one would like to have a measure of forces exerted by the growth on the tissue in order to study the feedback implied by mechanical growth control. This should be obtained non-invasively, such as to not disturb the developmental process. For this purpose, so far one only studies strain fields or strain rates of a tissue (10), which however only indirectly - via an elastic modulus - give information about the forces present. An alternative would be to determine stresses photo-elastically, i.e. by measuring the change in birefringence of a tissue in response to a stress (11).

Another instance, where mechanical forces have been implicated, is the growth of the wing imaginal disc of Drosophila (12; 13; 14). This is a precursor organ which will turn into the wing of the adult fly during metamorphosis (15). The wing imaginal disc forms a reasonably flat, epithelial tissue, which is made from two different layers of cells, the peripodial membrane and the columnar layer. These two layers are fundamentally different and most of the disc's mass is in the columnar layer, where cells are packed very tightly. This implies that the cell bodies form highly irregular structures, often packing several nuclei on top of each other (16). On the other hand, on the side of the columnar layer closest to the peripodial membrane, there is a rather ordered two dimensional surface. This is due to the presence of binding proteins only in this apical region of the cells, which gives structural stability to the cell contacts. Thus the topology and structural integrity of the wing imaginal disc can be described by a quasi two dimensional structure encompassing this apical region of the columnar layer. This has been modeled in a manner akin to two dimensional foams (17), which has shown that the mechanical properties of the tissue are important (16; 18).

While there have been many studies on the genetics of the growth regulation in the wing imaginal disc (20; 21), physical measurements are scarce. Experimentally, the work was limited to two cases. In the first case, laser ablation of cell contacts was used to asses the binding forces between cells in the tissue, which can be used as model inputs (18; 19). In the second case, photo-elasticity was used to asses the stresses present during development, where an inhomogeneous distribution of stresses inside the disc was found with high retardance in the centre of the wing pouch indicating compressional stress (22). Both this stress and its inhomogeneity increase as the wing disc grows. This is in agreement with the predictions of models of the size of a wing disc (13; 14). However in that work, the photo-elastic properties of the tissue were not

determined, such that a quantitative comparison with any model is not possible.

Here, we present a setup and initial measurements to determine the photo-elastic properties of wing disc tissue. Using a cantilever-type setup with which to apply controlled forces in the range of 1μN to 1mN in concurrent measurement of retardance, we are able to determine the overall tissue photo-elasticity. Due to possible inhomogeneities in the elastic properties of the tissue, local variations may exist that need further clarifying work. Below, we will present the forcing setup in detail as well as discuss its limitations and advantages. Moreover, we will discuss the principle behind the retardance measurements. These are carried out using a novel instrument capable of an accurate determination of the value of the retardance as well as its orientation in conjunction with a wide field microscope thus allowing fast measurements. After the presentation of these experimental setups, we will discuss initial measurements characterizing the photo-elastic response of the tissue and thus allowing a determination of an average photo-elastic constant. We conclude by comparing our findings with those previously obtained on retardance measurements in wing discs as well as general considerations of possible viscous properties of the wing disc and the corresponding time scales.

2 Experimental setup

The birefringent properties of the wing imaginal discs are measured using a Polscope from CRI (23). In this way, it is possible not only to measure the absolute value of the retardance, but also its orientation. The principle behind the measurement is to obtain a set of four intensities at different angles between the polarizer and analyzer and from this calculate the full polarization ellipsoid. This is similar to a setup previously developed for the direct study of magnetic fields using the Faraday effect (24). Since this allows a direct measurement of the polarization change of the light, as opposed to a quadratic one, which would be the case by a single intensity measurement, it yields much more accurate results (23; 24). In addition to the more accurate determination, the measurement of four different phase states allows a full determination of the polarization ellipsoid, which in the birefringence corresponds to a characterization of its orientation. In a photo-elastic experiment a change in birefringence, δn, is induced in the direction given by that of an applied stress (25), i.e.

$$\delta n = c(\sigma_1 - \sigma_2). \tag{1}$$

Here, σ_1, σ_2 are the principle components of the stress, which are at right angles. Since the change in birefringence can be measured in a particular direction, i.e. the one in which the stress is applied experimentally, this allows a direct determination of the photo-elastic constant c of the material. Below we will determine an averaged photo-elastic constant for tissue of the wing imaginal disc. Local inhomogeneities might lead to a distribution of photo-elastic constants, which can not be determined in this way. Such a local variation is however measurable when taking into account the change in orientation of the retardance signal in addition to its absolute value. This orientation would have to be correlated with the direction given by the external force. For this purpose, one would have to relate local variations in both retardance and orientation with the measured strain. Since we here are only interested in the macroscopic strain and its corresponding stress, we take the photo-elastic constant to be an effective constant of the whole tissue. Still, the changes in retardance we observe are correlated in orientation with the applied force indicating a certain degree of homogeneity of the tissue.

A schematic of the setup is drawn in Fig. 1. In order to apply a controlled force onto the wing imaginal discs, the discs were attached to two separate cover slips using poly-lysine solution. This leads to an electrostatic attraction of the tissue with the cover slip and thus an efficient fixation. While one of these cover slips is fixed, the other is attached to a sheet of spring steel at a right angle. Due to the geometric measures and the bending stiffness of the spring sheet, a calibrated force can be exerted on the cover slip and hence the wing disc by bending the spring sheet. For this purpose we have used a translation stage capable of resolving movements down to a micron with a travel range of several mm. Given the point of contact of the translation stage with the spring sheet, we can easily calculate the force exerted on the wing disc from classical elasticity (26):

$$F = \frac{6EI}{w^2(L-w)}d. \tag{2}$$

Here, $E = 2\times10^{11}$ Pa is the Young's modulus of the spring sheet, $I = a^3b/12$ is the area moment of inertia of the sheet with a thickness of $a = 40\mu$m and a width of $b = 1.1$cm. Furthermore, $L = 12$cm is the total length of the sheet and $w = 4$cm is the point of contact with the translation stage. Finally, d is the distance traveled by the translation stage. Taking these data on the spring sheet together yield a bending spring constant of 0.55N/m, such that the setup is capable of exerting forces between 1μN and several mN. This should be the right order of magnitude in order to significantly stretch the tissue of a wing disc.

In order to determine the photo-elastic response of the wing disc tissue, the polscope setup and the mechanical pulling setup have to be combined. Installing the polscope setup on an inverted microscope (Olympus IX-71) allows for such a combination due to the access for manipulation on top of the microscope objectives. Thus in our setup we are able to exert controlled forces onto wing disc tissue while simultaneously measuring the ensuing change in birefringence, both in the value of the retardance as well as in its orientation. However, to determine a photo-elastic constant, c, of the tissue, its geometry needs to be taken into account as well. This is because the photo-elastic constant relates an applied stress to the ensuing birefringence rather than an applied force to a measured retardance. The stress is given by the force divided by the cross-sectional area, $\sigma = F/(h \times y)$, with h the thickness of the disc and y its width. Moreover, the retardance is given by the birefringence times the thickness, $\delta = \delta n \times h$.

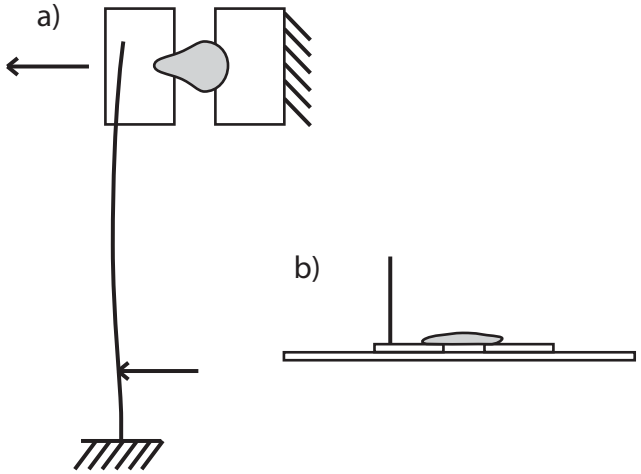

Figure 1. Schematic of the mechanical forcing setup. A top view is shown in a), while a side view is shown in b). The wing disc (grey) is attached to two glass cover slides, one of which is attached to a surface. The other cover slide is fixed to a spring sheet, which is forced by a translation stage at a given distance. This gives a controllable force ranging from 1μN to several mN, which is ideally suited to study epithelial tissues.

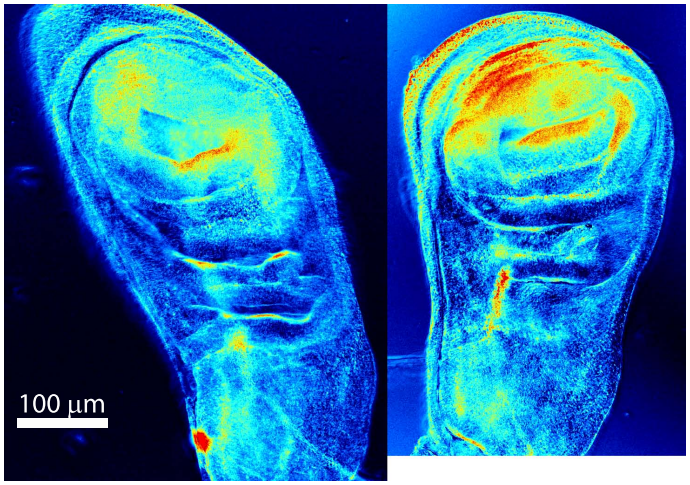

Figure 2. The retardance map of a wild type wing disc is shown on the right, whereas the same disc is shown after uncontrolled stretching on the left. The results are similar to those found previously on longer time scales and using a different setup. The colormap indicates retardance changing from 0 nm (black) to 10 nm (red). For a determination of photo-elastic properties, the stretching needs to be performed in a quantitative manner.

Therefore, the only additional quantity needed to determine the photo-elastic constant is the width of the stressed region of tissue as the thickness in the stress and the birefringence cancels. This width can be easily measured in our wide-field microscope.

3 Results

In order to test and calibrate the setup for retardance measurement, we have repeated the experiments of (22) and determined the retardance map both in untreated and manually stretched wing discs. The results are shown in Fig. 2. For the untreated disc, the peak retardance of 10 nm corresponds to the same value as found for this size in (22). Similarly, we find the same size dependence of the peak retardance and relaxation of the stress upon cutting of the discs. Moreover, as shown in Fig. 2, the results on the retardance reduction in the stretched disc are in good, quantitative agreement with the previous findings. In these unattached discs, the stretching changes the peak retardance by as much as 3 nm for a significant stretching. This results in a strain relative photo-elastic constant of $\sim 10^{-4}$, which considering typical photo-elastic materials is quite small (27). However, as mentioned above, in this stretching, the force is not known, such that no statements about the present stresses can be made.

For this purpose, we have used the pulling setup described above, compressing and stretching wing discs with a controlled force exerted by the spring sheet. Typical results for different mechanical forcing are shown in Fig. 3. Here, the retardance map is somewhat different from the unattached discs, which could be due to the fact that the attachment with poly-lysine also exerts mechanical stresses locally. In the figure, three different stages of the experiment can be seen, corresponding to a compression of the wing disc with a force of 300 μN (top), a slight stretching (80 μN - middle) and strong stretching at 500 μN (bottom). As can be seen from the different panels, the retardance in the three cases differs within the tissue. We have averaged the retardance over the central area of the pulled disc tissue and find values of 2.9 nm in the compressed case, 2.5 nm in the marginally stretched case and 2.1 nm in the fully stretched case. In all of the cases, the orientation of the retardance is roughly parallel to the direction of the force, indicating that the change in retardance can be directly related to the applied force. Given the width of the stretched region of $y \sim 200\mu$m, the photo-elastic constant is obtained from ratio of the change in birefringence to that in stress (Eq. 1). In combination with the geometric relations given above this is related to the ratio of retardance change $\Delta\delta$, to the change in force ΔF:

$$c = y\Delta\delta/\Delta F = 2 \times 10^{-10} Pa^{-1}, \qquad (3)$$

both for compression and stretching. This is comparable to typical values of photo-elastic constants for crystalline materials (27; 28). The fact that the strain relative photo-elastic constant is much smaller than typical materials points to the softness of the tissue and the correspondingly small elastic modulus.

In some of our experiments, the force of attachment on the cover slide was comparable to the force exerted by the spring sheet. This led to a detachment of the wing disc after having been subject to a stretching force for several minutes to half an hour. As can be seen from Fig. 4, such detached wing discs revert to their original size, which

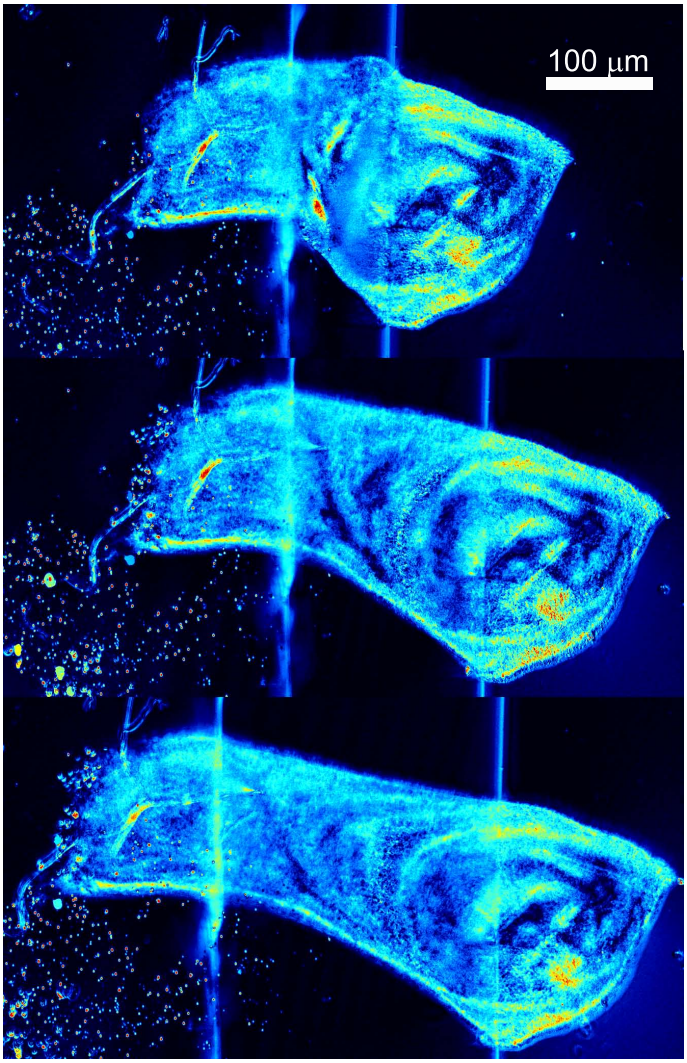

Figure 3. The retardance map of a wing disc at different levels of stretching in the y-direction. The scale bar indicates a distance of 100 μm and the colormap indicates retardance, changing from 0 nm (black) to 10 nm (red). In the top figure, the disc is compressed with a force of 300 μN, while in the middle panel the disc is roughly in its initial state with a stretching force of about 80 μN. The bottom figure shows a stretched wing disc at a force of 500 μN. Note that for an accurate determination of the changes in retardance that can be seen in the figure, proper averages over the stretched tissues need to be taken. The resulting differences are of the order of 0.5 nm, with an increase in retardance for compressional stress and a decrease for tensional stress.

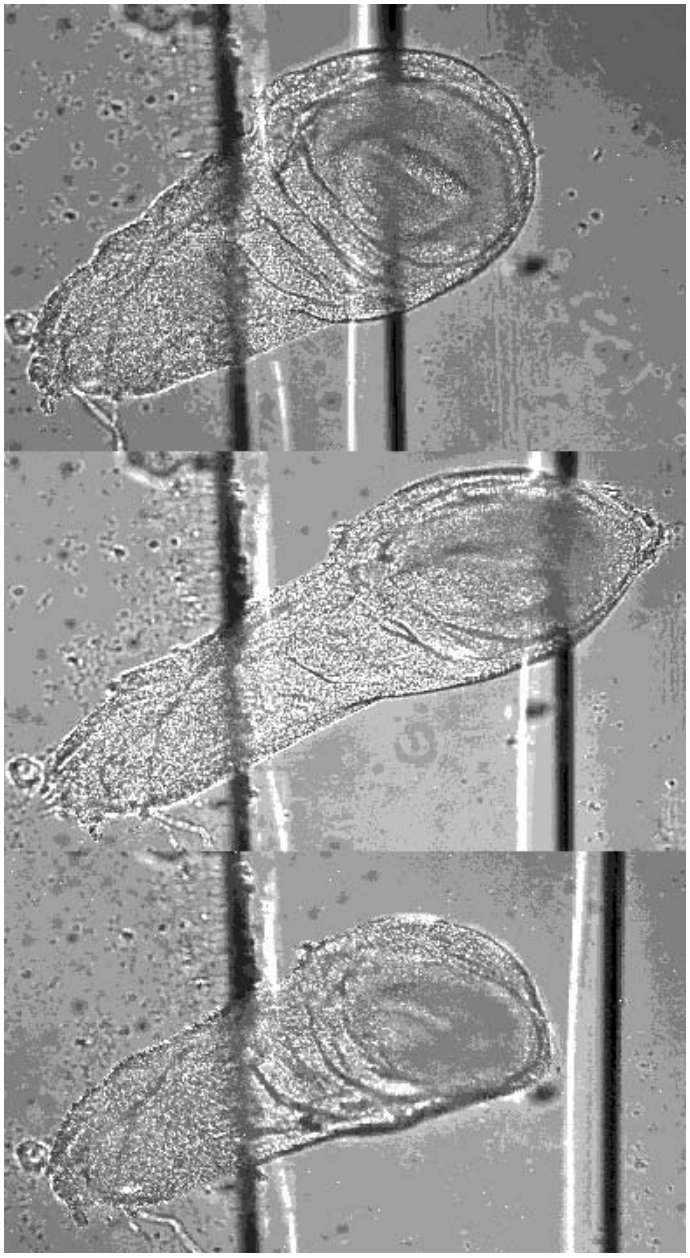

Figure 4. A stretched wing disc that has been detached from the cover slide (bottom). As can be seen from comparison with the situation before stretching (top), the disc reverts to its original shape and size in spite of having been stretched substantially, shown in the middle panel. The discrepancy in form is explained by the fact that the unattached part of the disc is free to move n the z-direction thus losing the focus. This indicates that on the corresponding time scale of half an hour and for strains as big as 0.3, the disc behaves elastically.

takes place over the course of 2-3 seconds. The slight difference in appearance visible in Fig. 4 is due to the fact that the unattached side of the disc can move in the z-direction bringing it out of focus and thus changing the form somewhat. This implies that on the time-scale of half an hour, the tissue does act elastically. In fact, a force extension curve of a typical wing disc is rather linear, as can be seen in Fig. 5, with an effective spring constant of 5(1)N/m. This directly corresponds to a Young's modulus of the order of 10^5 Pa. Compared to other tissues, which have been studied experimentally (7; 8; 9), this is rather large implying a more elastic behaviour of wing discs than of other tissues. It should be noted however that all of these investigations were done on embryonic tissues, which is not the case for wing imaginal discs. For instance, the mechanical fluctuations in the larva when feeding and moving are much higher than in the embryo thus invoking

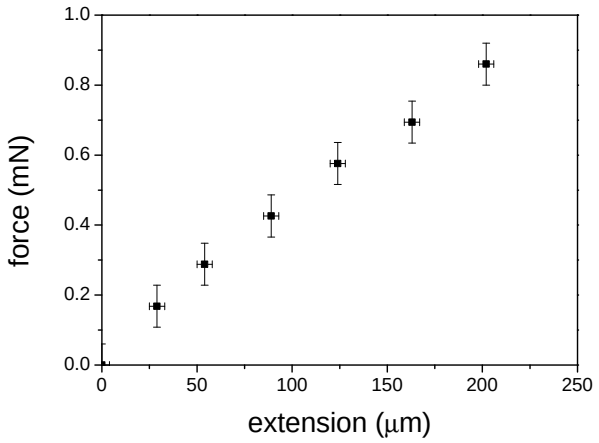

Figure 5. Force extension curve of a wing imaginal disc. The extension is taken starting from the relaxed state. This implies a high spring constant of wing disc tissue as compared to other samples (7; 8; 9).

stronger tissues. This is corroborated by moduli of adult tissues, such as blood vessels, skin or muscle, which range between 10^5 and 10^6 Pa (29; 30), comparable to our results.

4 Conclusions

We have presented a setup for the determination of elastic properties of epithelial tissues, such as that of the wing imaginal disc of Drosophila, where we have also performed initial experiments. These mechanical properties include photo-elastic properties due to the combination of the setup with an automated polarization microscope capable of determining the retardance of a sample to high accuracy. For the wing imaginal disc, we have found a value of the photo-elastic constant of $2\times10^{-10}\mathrm{Pa}^{-1}$, which is comparable to typical photo-elastic materials. Given the softness of the wing disc tissue, the relative photo-elasticity is quite small and would be of the order of 10^{-4}. Furthermore, we have determined an effective spring constant of the wing disc, where we find a value of 5(1)N/m, which is considerably higher than values for other, embryonic, tissues in the literature (7; 9) and lies more in the range of adult tissues or muscle (29; 30). This could imply that the wing disc acts more elastically than embryonic tissues, which is indeed consistent with our observation that a detached wing disc reverts back to its original shape even after having been stretched for almost half an hour. This much more elastic behaviour might be connected to the mechanical feedback implied in the size models suggesting a role for forces that are built up during development (13; 14). For a rather viscous material, such as those found in embyonic tissues (7; 9), it would be much more difficult to arrange for this. A detailed study of the molecular mechanisms behind this elasticity remains for future investigations.

5 Acknowledgements

This work was supported by SystemsX.ch in the framework of the WingX RTD, as well as the University research priority programme in systems biology of the University of Zurich. We would also like to thank Tinri Aegerter-Wilmsen and Ulrike Nienhaus for fruitful discussions as well as Michael Schindlberger for initial work on the mechanical force setup described here.

References

1. D'Arcy Wentworth Thompson, *On Growth and Form*, Dover (1959).
2. D.E. Ingber, FASEB Journal **20**, 811 (2006).
3. O. Hamant, M.G. Heisler, H. Jonsson, P. Krupinski, M. Uyttewaal, P. Bokov, F. Corson, P. Sahlin, A. Boudaoud, E.M. Meyerowitz, Y. Couder, and J. Traas, Science **322**, 1650 (2008).
4. E. Caussinius, J. Colombelli, and M. Affolter, Curr. Biology **18**, 1727 (2008).
5. R.B. Martin and D.L. Boardman, J. Biomech. **26**, 1047 (1993).
6. J. Kahn, Y. Schwartz, E. Blitz, A. Sharir, D.A. Breitel, R. Rattenbach, F. Relaix, P. Maire, R.B. Rountree, D.M. Kingsley, and E. Zelzer, Dev. Cell **16**, 734 (2009).
7. R.A. Foty, C.M. Pfleger, G. Forgacs, and M.S. Steinberg, Development **122**, 1611 (1996).
8. E.M. Schötz, R.D. Burdine, F. Jülicher, M.S. Steinberg, C.P. Heisenberg, and R.A. Foty, HFSP Journal **2**, 42 (2008).
9. C. Wiebe and G.w. Brodland, J. of Biomechanics **38**, 2087 (2005).
10. N. Gorfinkiel, G.B. Blanchard, R.J. Adams, and A. Martinez Arias, Development **136**, 1889 (2009).
11. T.S. Majmudar and R.P. Behringer, Nature **435**, 1079 (2005).
12. B.I. Shraiman, Proc. Natl. Acad. Sci. USA **102**, 3318 (2005).
13. L. Hufnagel, A.A. Teleman, H. Rouault, S.M. Cohen, and B.I. Shraiman, Proc. Natl. Acad. Sci. USA **104**, 3835 (2007).
14. T. Aegerter-Wilmsen, C.M. Aegerter, E. Hafen, and K. Basler, Mechanisms of Development **124**, 318 (2007).
15. L. Wolpert, *Principles of Development*, Oxford Univ. Press (2006).
16. T. Aegerter-Wilmsen, A.C. Smith, A.C. Christen, C.M. Aegerter, E. Hafen, and K. Basler, Development **137**, 499 (2010).
17. M. Aubouy, Y. Jiang, J.A. Glazier, and F. Graner, Granular Matter **5**, 67 (2003).
18. R. Farhadifar, J.-C. Röper, B. Aigouy, S. Eaton, and F. Jülicher, Curr. Biology **17**, 2095 (2007).

19. K.P. Landsberg, R. Farhadifar, J. Ranft, D. Umetsu, T.J. Widmann, T. Bittig, F. Jülicher, and C. Dahmann, Mechanisms of Development **126**, S77 (2009).
20. S.M. Cohen, in *The Development of Drosophila melanogaster*, M. Bate and A. Martinez Arias, eds., Cold Spring Harbor Laboratory Press: Cold Spring Harbor, 747 (1993).
21. M. Affolter and K. Basler, Nat Rev Genet **8**, 663 (2007).
22. U. Nienhaus, T. Aegerter-Wilmsen, and C.M. Aegerter, Mechanisms of Development **126**, 943 (2009).
23. M. Shribak and R. Oldenbourg, App. Optics **42**, 3009 (2003).
24. R.J. Wijngaarden, M.S. Welling, C.M. Aegerter, and K. Heek. NATO Science Series II: **142**, 61 (2004).
25. M.M. Frocht, *Photoelasticity, Volume 1 and 2*, John Wiley and Sons, Inc., New York (1941 and 1948).
26. L.D. Landau and E.M. Lifshitz, *Course on theoretical Physics VII: Elasticity*, Oxford (1960).
27. *Handbook of Chemistry and Physics*, 82nd ed., CRC Press (2001).
28. T.S. Narasimhamurty, Phxs. Rev. **186**, 945 (1969).
29. J.Zhou and Y.C. Fung, Proc. Nat. Ac. Sci. USA **94**, 14255 (1997).
30. M.R. Neidert, E.S. Lee, T.R. Oegema, and R.T. Tranquillo, Biomaterials **23**, 3717 (2002).